Hybrid ring-mesh topology enabled 16×100 Gbps integrated MDM-OCDMA PON/FSO system incorporating a new MFRS code

MEET KUMARI[1,*], SHONAK BANSAL[1], GAURAV BATHLA[2]
[1]*Department of ECE, UIE, Chandigarh University, Gharuan, Mohali, Punjab-140413, India*
[2]*Department of CSE, UIE, Chandigarh University, Gharuan, Mohali, Punjab-140413, India*

A symmetric and bidirectional 16×100 Gbps integrated mode division multiplexing (MDM)-optical code division multiple access passive optical network (OCDMA-PON) with free space optics (FSO) system is presented in this paper. A ring-mesh topology is incorporated to enhance system capacity under disaster conditions. The results depict that the system can provide faithful 75 km multimode fiber and 2800 m FSO range using a new two-dimensional modified fixed right shifting code. The system supporting 190 users can also sustain high gain, low noise figure and high signal to noise ratio. Compared to literature this system offers better performance.

(Received September 30, 2023; accepted June 5, 2024)

Keywords: FSO, TWDM, OCDMA, PON, MDM

1. Introduction

With rapidly elevating fifth generation (5G) networks, machine to machine communication and internet of things, attention is promptly focused on future generation paradigms comprising sixth generation (6G) networks as well as the tactile internet. Wireless and wired communication networks will lead to promptly evolve both in terms of capabilities and their architectures to sustain the surge in latency-sensitive robot application like augmented reality, industry automation, intelligent systems and telesurgery [1]. However, 5G networks are deployed effectively throughout the world, various groups are still working on the 6G wireless systems and high capacity next generation passive optical networks (NGPONs) [2].

Accordingly, 5G fronthaul technology has endorsed the NGPON stage 2 (NGPON2) architecture having several possible configurations like 50 gigabit PON (50G-PON), long reach PON (LRPON) and time and wavelength division multiplexing (TWDM) PON [2]. Among the possible architectures, TWDM-PON which is most suitable to fulfill the fronthaul requirements is considered as a favorable fronthaul solution for 5G, thanks to its low energy consumption, low cost as well as abundant bandwidth. Besides, TWDM-PON fronthaul, the network feasibility is confirmed, can conform the bandwidth greater than time division multiplexing (TDM) [3].

On the other hand, optical code division multiple access (OCDMA) offers additional dimension of multiple access, other than optical frequency and time domains. Regrettably, it remained outside the major stream of optical access networks due to immature optical devices, which are restrictive to OCDMA, like optical en-/decoder as well as optical thresholding devices. Also, the crosstalk among several users sharing the single channel, called as multiple access interface (MAI) as well as beat noise is the primary source of bit errors. The diminution of beat noise and MAI are main challenges to make OCDMA a practical selection for NGPON2 based system. Thus, being motivated by the hybrid TWDM-OCDMA PON now acquires reconsidering as a multiple-access approach for NGPON2 networks [4]. Also, the system performance can be significantly improved by choosing the right OCDMA code. Recently, in [5], NGPON basics OCDMA hybrid fiber-wireless system using maximal length sequence serving six users at 160Gbps transmission rate is realized. Also, in [6], OCDMA PON using super-structured fiber Bragg grating en-/decoder over 50 km distance with 160 Gbps total capacity is developed. In another work [7], hybrid OCDMA and wavelength division multiplexing (WDM) system over 22 km transmission at 1.25 Gbps data rate is proposed. In [8], hybrid TWDM and OCDMA-WDM system using modified quadratic congruence at 160/40Gbps transmission rate over 70 km fiber is demonstrated.

Again mode division multiplexing (MDM) is a possible multiplexing approach which uses distinct light modes of same wavelength to assistance the capacity of NGPON2. In a fiber core, the number of signals can be enhanced by utilizing MDM technique. MDM utilizes the distinct modes of multi-/few mode fiber as uncommon data channels [9]. Recently, in [10], a successful transmission at 120 Gbps capacity in a hybrid MDM-WDM as well as radio over FSO system over 80 km FSO range considering strong atmospheric scenario is reported. An effective 80 Gbps transmission over 50 km FSO link

concerning fog weather is presented [11]. In another work [12], a 200 Gbps data transmission over 1.7 km MDM-FSO link range is reported.

Although, PONs can be utilized for various applications in industry, office, army sectors and business which generally require higher level of link protection along with the assurance of maximum functionality of whole network structure. For this it is clear that it is important to develop effective backup and protection mechanisms to protect serious optical network units (ONUs) and optical distribution network (ODN) in PONs. A standard ODN generally has a star topology with a single linked point or a tree topology having several linked points, which makes optical line terminal (OLT) methods complex and difficult. In these topologies, backup cannot be quite reliable as the whole network structure is nevertheless vulnerable in various situations e.g. floods, power failure, terrorist actions etc. Besides this, the ring topology is used to protect sensitive applications of PONs. But due the presences of passive splitters' high insertion loss cause high attenuation and thus ring topology is mostly restricted in local area networks [13]. By allocating two directed fibre links, OLT, in contrast to the ring topology, directly connects every linked ONU. However, survival necessitates a uniform interface for communication that allows for a single control module [14]. In literature, numerous topologies have been presented previously that are capable to fulfill users' demands. A tree-basics PON employing self-restroable apparatus is investigated in [15], which provides less restoration time of 7ms for PON protection. In [16], a ring topology basics WDM-PON is prsensented to analyze the system reliability with network scalibility. It is shown that minimum -26 dBm receeiver sensivity can be obtained supporting maxumim eight number of remote nodes (RNs). Also, in [17], a ring-basics PON architecture incorporating asymemetric passive splitters is experimental demonstrated to provide traffic full restoration if an OLT is failed. Additionally, an integrated ring-tree toplogy basics WDM system sustaining 64 consumers at 60Gbps data rate is reported in [18].

However, from these topologies it is clear that there is a requirement for more work providing high data rate, transmission range both using wired and wireless access and large number of users. Therefore, in this work, hybrid ring-star topology based an integrated MDM-NGPON2/FSO system using a two-dimensional modified fixed right shifting (2D-MFRS) code for 5G fronthaul infrastructure is presented. In this work, bidirectional hybrid fiber-FSO links are utilized for data transmission concerning Gamma Gamma (GG) and distinct weather conditions. The combination of fiber with FSO is becoming a promising solution for providing low energy consumption, high bandwidth, reliable, secure, low maintenance and cost-effective services on internet [19]. Hybrid fiber/FSO link offers best solutions against fiber breakage over conventional fiber as well as radio frequency communication [19]. Recently, an integrated PON-FSO over 300 m FSO with 25 km fiber range at 10 Gbps throughput is demonstrated [20]. To further enhance the FSO range upto 1.4 km, a hybrid fiber-FSO system at 1Gbps throughput over 20 km fiber is also presented [21].

High-bandwidth, flexible, high-speed, low cost as well as anytime-anywhere communication technology permits business users to access a wide range of services/resources, including education, e-commerce, public safety, entertainment, healthcare scenario and many more [22]. The novelty of this work is that hybrid MDM-NGPON2/FSO system is fault tolerant and more robust compared to conventional PONs owing to wireless end self-healing capability. As there are some concerns in 5G network in which fiber connections are impossible or in the rural areas which lacks in optical fiber infrastructure, thus long-reach FSO communication can be utilized in such scenarios. Again, the hybrid fiber-FSO based networks are critically hindered by immense failures due to malicious human activities, weather-related disruptions and natural disasters. Therefore, there is a need to focus on these scenarios especially for 5G fronthaul access networks to improve the disaster resilience against the several classes of disaster events. Moreover, hybrid ring-mesh topology further improves the architecture capacity multiple times as compared to conventional topologies used in PONs. In this work, hybrid NG-PON2/OCDMA PON comprises the integration of TWDM and two-dimensional modified fixed right shifting (2D-MFRS) code employed OCDMA multiplexing schemes over hybrid fiber-FSO links. This architecture permits high speed, high bandwidth, flexible, reliable, long-reach, 'pay-as-you-grow', easy upgradeable, low cost, mobile, handling large number of users and secure data transmission under fiber channel impairments, weak-to-strong turbulent and several weather conditions of FSO link.

In this paper, hybrid ring-mesh topology based NGPON2-OCDMA/FSO system using 2D-MFRS code for 5G fronthaul network is proposed and investigated. Major contributions are as:

a) However, hybrid PON/FSO systems have been studied over the last decade, but the hybrid NGPON2/FSO system based on hybrid ring-mesh topology is reported first time in this work.
b) Proactive protection architecture for hybrid fiber-FSO based network against failures arises from unpredictable disasters is investigated.
c) A new OCDMA code i.e. 2D-MFRS code for secure transmission is also employed.
d) Performance of system is validated by comparing proposed work with earlier work.

This work is structured as: Proposed architecture is presented in Section 2. Measured results with discussion are reported in Section 3 and conclusion is presented in Section 4.

2. Proposed architecture

Fig. 1 indicates the semantic diagram of hybrid ring-mesh topology based integrated MDM-NGPON2/FSO system for 5G fronthaul applications. In this architecture,

OLT is positioned at centre of bidirectional ring structure via 'n' number of hybrid fiber-FSO links to RNs. Each RN is further connected to two ONUs as end nodes for internet of things, artificial intelligence, smart agriculture, transportation, healthcare systems, industry automation and many more applications.

Different downstream (DS) as well as upstream (US) from λ_1 to λ_n are employed in a hybrid ring-mesh architecture from OLT to RNs and vice versa. OLT facilitates inter/intra-RN communication, identification as well as control facilities [23].

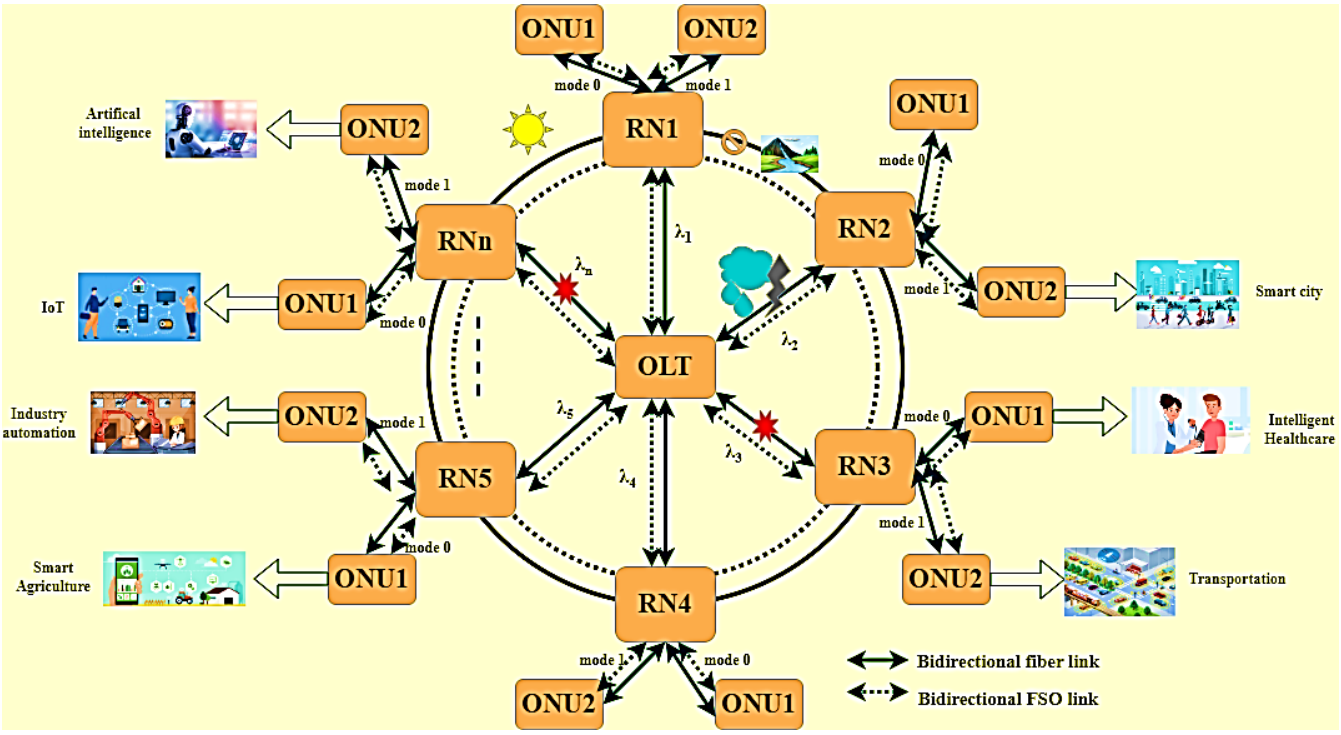

Fig. 1. Semantic diagram of hybrid ring-mesh topology based integrated MDM-NGPON2/FSO system (color online)

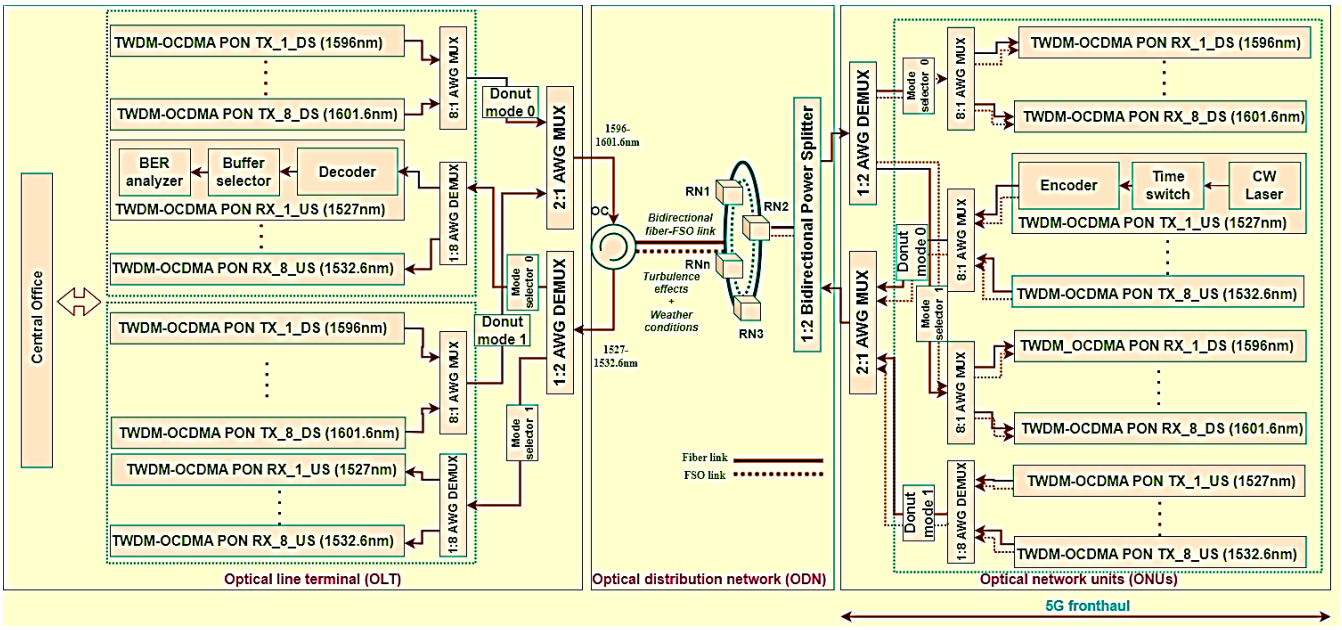

(a)

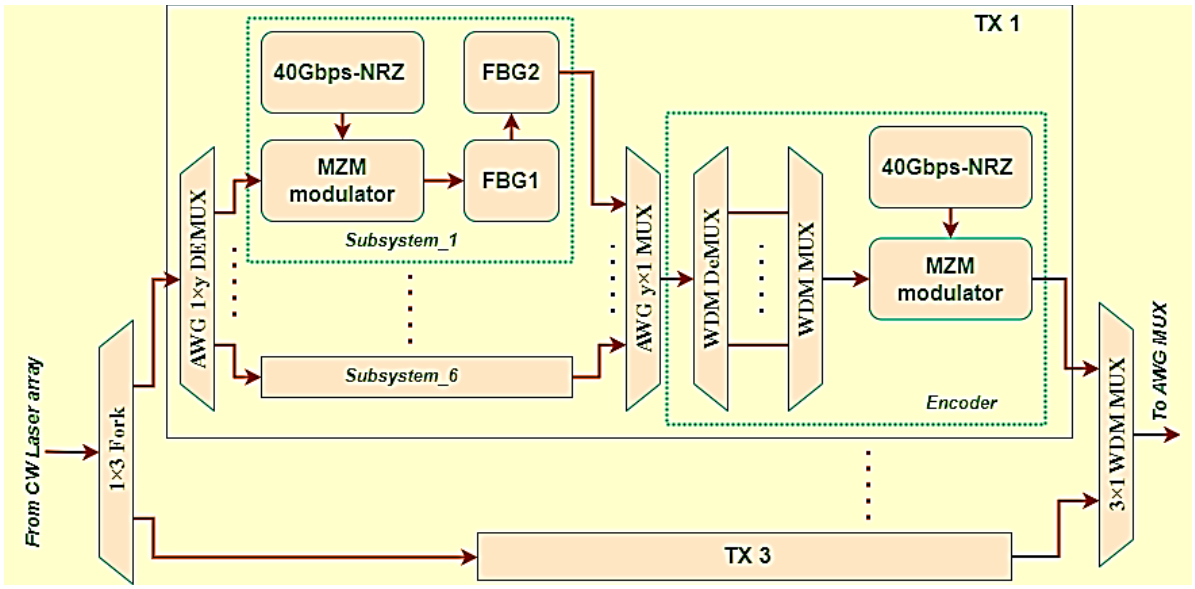

(b)

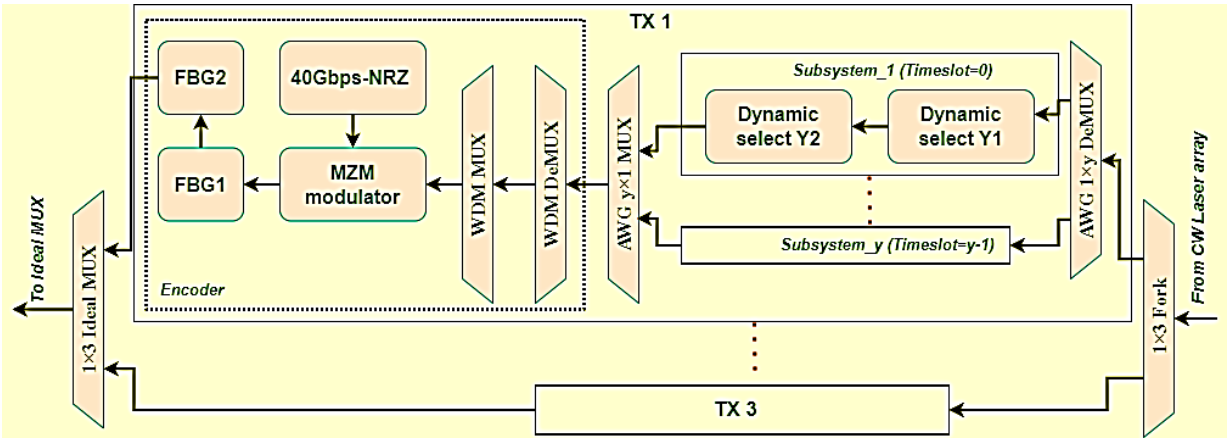

(c)

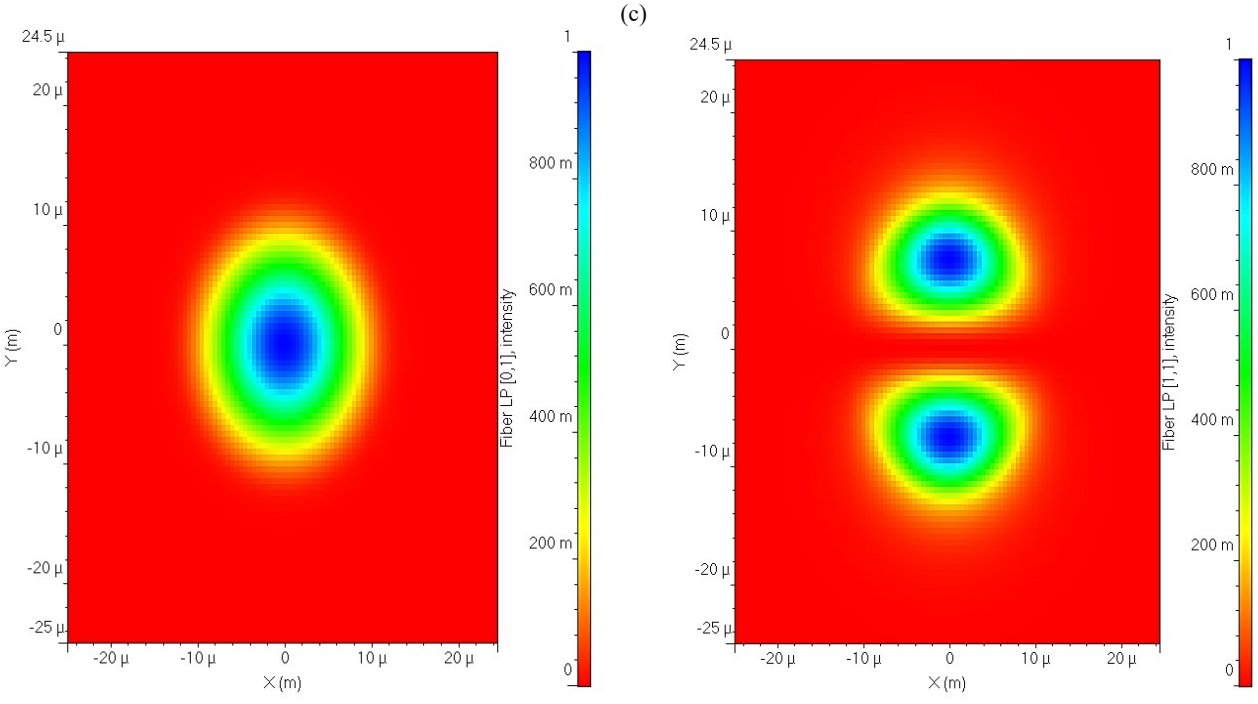

(d) (e)

Fig. 2. (a) Block diagram of 5G fronthaul hybrid ring-mesh topology based integrated MDM-NGPON2/FSO system (b) DS Tx section, (c) US Tx section, generated (d) donut mode 0 and (e) donut mode 1 (color online)

The data transmission, regeneration as well as rebroadcasting in ring structure is carried out either anti-clockwise or clockwise. Further, two donut modes viz. mode 0 and mode 1 are utilized for two ONUs connected at each RN. To secure the system, 2D-MFRS OCDMA code is employed at DS/US transceivers. The primary benefit of this architecture is to use FSO links capacity for ink failure scenario under various disaster conditions and the data will be routed from broken or failed path onto an alternative linked path which surrounds the OLT, or a nearby RN or ONU connection [23].

Fig. 2(a) illustrates the block diagram of bidirectional hybrid ring-mesh architecture based 16×40 Gbps integrated TWDM/OCDMA PON with FSO system using 2D-MFRS code. Two donut modes 0 and 1 are employed for data transmission in the proposed system via hybrid FSO-fiber links. As depicted in figure, eight transceivers in DS and eight transceivers in US operating at mode 0 and mode 1 produces different signals for several 5G applications. At OLT, eight DS hybrid TWDM-OCDMA multiplexed signals at 8:1 array waveguide grading (AWG) MUX after operating separately at mode 0 and mode 1 are multiplexed via 2:1 AWG MUX are passed through ODN section. The ODN section incorporates a bidirectional optical circulator; a bidirectional hybrid multimode fiber-FSO link and ring shaped multiple RNs. Here, hybrid fiber-FSO is linked bidirectional considering fiber impairments and FSO atmospheric conditions. Also, each RN is connected to a 2:1 bidirectional splitter for DS and US transmission. In the same way, US coded signals are passed via ODN section and then detected at OLT [24].

Fig. 2(b) depicts he block diagram of a DS transmitter (Tx) section for different 2D-MFRS OCDMA users, where OLT and ONU units comprise three pairs of Txs and receivers (Rxs) for three coded users. As depicted in diagram, for a single DS Tx section of hybrid TWDM-OCDMA PON/FSO, eight continuous wave lasers generates eight wavelengths (1596, 1596.8, 1597.6, 1598.4, 1599.2, 1600, 1600.8 and 1601.6 nm) which are fed into a n:1 AWG MUX (n=8) followed by a 1×3 Fork for three DS Txs. Further, a Tx section employs, a 1×y AWG DEMUX having y=8 input signals. Then, obtained outputs from AWG DEMUX are transferred to a Subsystem_1 to Subsystem_6. A Subsystem consists of a pseudo random bit sequence with non return to zero (PRBS-NRZ) bit sequence to be modulated via a mach zehnder modulator (MZM) with input signals. For signal encoding, two consecutive fiber Bragg grading (FBG) i.e. FBG1 and FBG2 components are utilized. A y×1 AWG MUX is incorporated to multiplexed the modulated signals from Subsystems to encoder section. Here, each encoder comprises a 1×6 WDM DEMUX which is followed by a 6×1 WDM MUX to transfer the data into MZM to re-modulated along with PRBS-NRZ at 40 Gbps traffic rate. The generated coded signals are multiplexed by a 3×1 WDM MUX and then transmitted over bidirectional hybrid fiber-FSO links. Reverse process is performed to decode the signals via decoder followed by photo-detector (PD), filter and BER analyzer at ONUs side [24].

Fig. 2(c) illustrates a single US Tx section of hybrid TWDM-OCDMA PON incorporating 2D-MFRS code with eight US wavelengths (1527, 1527.8, 1528.6, 1529.4, 1530.2, 1531 and 1531.8, 1532.6 nm) generated by eight laser diodes. For US transmission, two dynamic Y select components are employed to generate signals at distinct time slots from 0 to 7. Like DS transmission, US coded signals are produced and detected at Rx side. The encoded signals generated by each encoder section using two FBGs, MZM and PRBS-NRZ are detected at OLT side after transmission over hybrid fiber-FSO links. The received US signals are passed through buffer selector via decoder and then anlayzed through bit error rate (BER) analyzer. Fig. 2(d) and 2(e) indicate generated donut modes 0 & 1 respectively. Mode selectors 0 as well as 1 are utilized to select the mode 0 and 1 respectively at both Tx and Rx side. Buffer selector is incorporated to select the latest iteration of US signals [8].

Table 1 illustrates the 2D-MFRS code design used in proposed architecture and it comprises two code sequences X and Y having code weight of 3. In addition, for code sequences X and Y, the number of active subscribers in spectral as well as spatial domains is 6 and 4 respectively. Table 2 various performance parameters used in architecture. Table 2 indicates the parameters of proposed architecture.

Table 1. 2D-MFRS code design [25]

	$Y_1 = [0\ 0\ 0\ 0\ 0\ 0\ 1\ 0\ 1\ 1]$	$Y_2 = [0\ 0\ 0\ 0\ 0\ 1\ 0\ 1\ 1\ 0]$	$Y_3 = [0\ 0\ 0\ 1\ 0\ 1\ 1\ 0\ 0]$	$Y_4 = [0\ 0\ 1\ 0\ 1\ 1\ 0\ 0\ 0]$	$Y_5 = [0\ 1\ 0\ 1\ 1\ 0\ 0\ 0\ 0]$	$Y_6 = [1\ 0\ 1\ 1\ 0\ 0\ 0\ 0\ 0]$
$X_1^T = [0\ 0\ 1\ 0\ 1\ 1\ 0]$						
$X_2^T = [0\ 0\ 1\ 0\ 1\ 1\ 0]$						
$X_3^T = [0\ 1\ 0\ 1\ 1\ 0\ 0]$						
$X_4^T = [1\ 0\ 1\ 1\ 0\ 0\ 0]$						

Table 2. Performance parameters [8,23]

Parameters	Values
Wavelengths	1596-1601.6 nm (for DS), 1527-1532.6 nm (for US)
Throughput	40-100 Gbps
Input power	10 dBm (for DS), 0 dBm (for US)
Reference wavelength	1550 nm
No. of channels	16
MMF length	10-80 km
FSO range	100-3100 m
Tx/Rx aperture diameter	20 cm
Beam Divergence	0.25×10^{-3} rad
Dispersion	16 ps/nm×km
Attenuation	0.20 dB/km
Clear air	0.35 dB/km
Fog	4.2 dB/km
Rain	6.2 dB/km
Snow	38.6 dB/km
Turbulence effects	10^{-17} $m^{-2/3}$ (weak), 10^{-14} $m^{-2/3}$ (moderate), 10^{-13} $m^{-2/3}$ (strong)
Scintillation model	Gamma-Gamma

3. Results and analysis

To design the proposed architecture Optiwave simulation tool OptiSystem is used and also to evaluate the performance architecture in BER under various FSO link disturbances. Clear air as well as weak turbulence conditions is considered for multi-beam FSO links if not stated [26–28].

Mathematically, total BER due to MDM and hybrid TWDM-OCDMA schemes using FSO link is evaluated as [8,23]:

$$BER_{Total} = 0.5erfc\left(\frac{SNR_0}{\sqrt{2}}\right) + 0.5\int_0^{\infty} f_{g_a}(g_a)\, erfc\left(\frac{\langle SNR\rangle s_i}{2\sqrt{2}\langle i_{s_i}\rangle}\right) ds_i \quad (1)$$

where $erfc(.)$ depicts complementary error function, SNR_0 is output signal to noise ratio, $f_{g_a}$is GG channel distribution, g_a means atmospheric disturbance, $\langle SNR\rangle$ mean signal to noise ratio, s_i is signal strength and i_{s_i} is signal current at PD.

Fig. 3(a)-3(f) indicate the system performance for varied FSO link with fixed 40 km fiber at symmetric 40 Gbps transmission rate under weak-to-strong turbulence, separate as well as combination of fog, rain, snow weather conditions operating at mode 0 and mode 1. It is clear that with increase in transmission range the impact of channel disturbances improves concerning all environment conditions in both US and US modes signals. Out of all weather conditions, after clear air with no turbulent condition, fog shows best performance over rain followed by snow and the combined fog+rain+snow climate condition. Mode 0 transmission signals perform optimum over mode 1 signals. Fig. 3(a) and 3(b) illustrate that maximum faithful FSO range for US mode 0 and DS mode 0 signals is 2800 and 2500 m respectively at BER limit of 10^{-9}, under weak turbulent and fog condition. Also, FSO ranges reduce to 2350 and 2200 m for US mode 0 and DS mode 0 signals respectively, under moderate turbulent and fog condition as depicted in Fig. 3(c) and 3(d). However, the worst FSO range under strong turbulent can be obtained upto 2150 m for US mode 0 and 1900 m for DS mode 0 concerning fog climate condition as shown in Fig. 3(e) and 3(f).

Besides this, the wide open eye patterns under weak, moderate and strong turbulent impact for fog condition for mode 0 signal in DS and US transmissions indicate the superiority of signals for US mode 0 signals under weak over others signals.

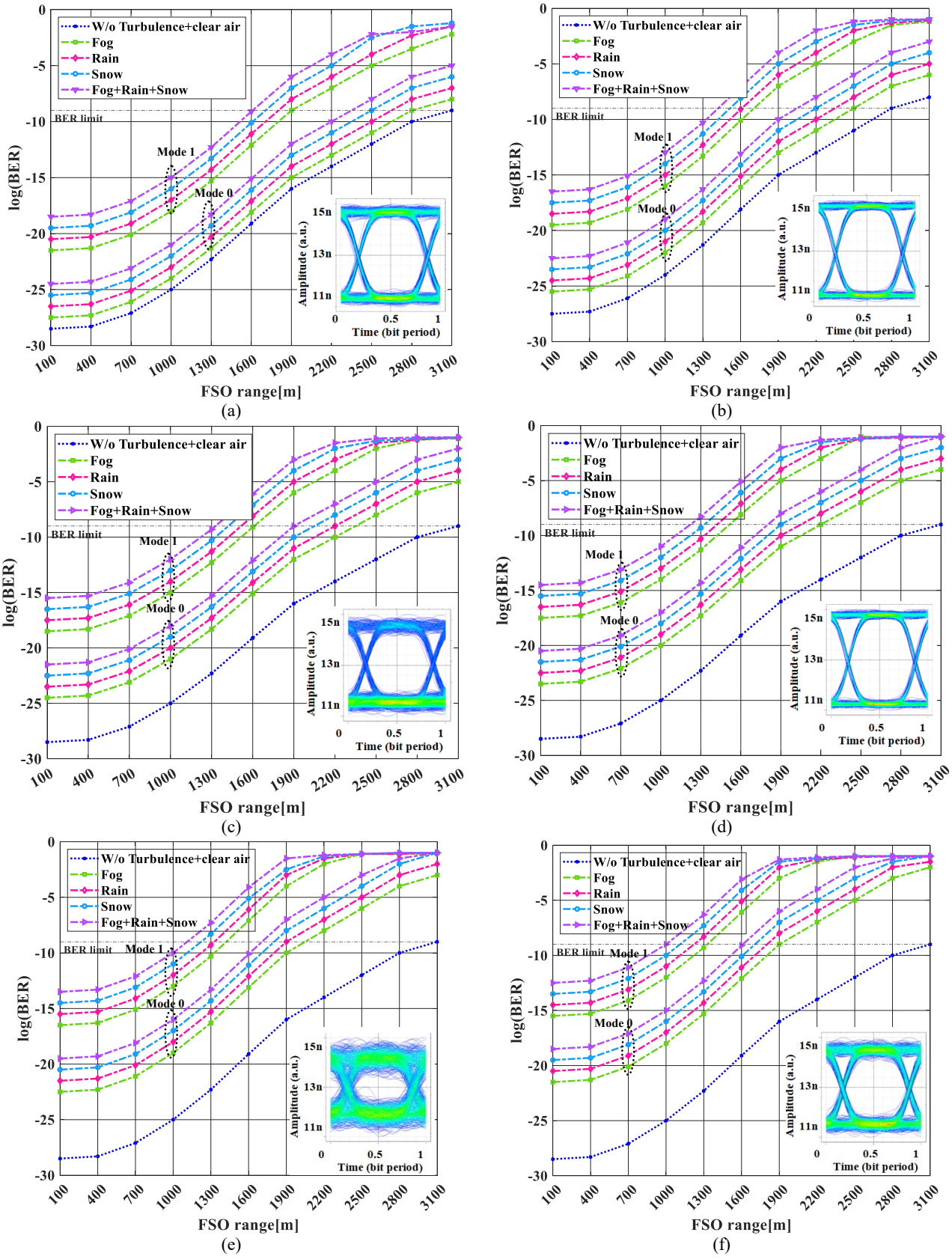

Fig. 3. Measured BER for varied FSO range under different weather conditions operating at mode 0 and mode 1 for (a) US in weak, (b) DS in weak, (c) US in moderate, (d) DS in moderate, (e) US in strong and (f) DS in strong turbulent conditions at fixed 40 km fiber length; Insets: corresponding eye patterns at BER limit of mode 0 signal under fog climate (color online)

Tables 3 and 4 illustrate the performance evaluation of DS and US transmission signals respectively, under distinct modes and FSO channel disturbances. From tables it is clear that FSO range can vary from 2800 to 1000 m under weak-to-strong turbulence and fog+rain+snow weather condition.

Table 3. Maximum obtained FSO range in DS transmission under different turbulent and weather conditions @10^{-9} BER

Weather condition	Max. FSO range (m)					
	Weak turbulent		Moderate turbulent		Strong turbulent	
	Mode 0	Mode 1	Mode 0	Mode 1	Mode 0	Mode 1
Fog	2500	1700	2200	1550	1900	1300
Rain	2350	1600	2050	1450	1850	1250
Snow	2200	1550	1900	1300	1700	1100
Fog+Rain+Snow	2050	1450	1850	1250	1600	1000

Table 4. Maximum obtained FSO range in US transmission under different turbulent and weather conditions @10^{-9} BER

Weather condition	Max. FSO range (m)					
	Weak turbulent		Moderate turbulent		Strong turbulent	
	Mode 0	Mode 1	Mode 0	Mode 1	Mode 0	Mode 1
Fog	2800	1900	2350	1600	2050	1400
Rain	2650	1850	2200	1550	1900	1300
Snow	2500	1700	2050	1400	1850	1250
Fog+Rain+Snow	2350	1600	1900	1300	1700	1100

An integrated fiber and FSO link is used in architecture taking into account GG distribution model as [24]:

$$S_a(a) = \frac{2(gh)^{\left(\frac{g+h}{2}\right)}}{\Gamma(g)\Gamma(h)} . a^{\left(\frac{g+h}{2}\right)-1} J_{g-h}\left[2(gha)^{\frac{1}{2}}\right] \quad (2)$$

where a means atmospheric turbulence, g as well as h define large plus small-scale effective eddies channel parameter values considerably. $\Gamma(.)$ as well as J_{g-h} indicate Gamma function as well as modified Bessel function having order of $(g-h)$ respectively. Here, g and h are defined as [24]:

$$g = \left[exp\left\{\frac{0.49b_0^2}{\left(1+0.18d^2+0.56b_0^{12/5}\right)^{7/6}}\right\} - 1\right]^{-1} \quad (3)$$

and

$$h = \left[exp\left\{\frac{0.51b_0^2\left(1+0.18d^2+0.56b_0^{12/5}\right)^{-5/6}}{\left(1+0.90d^2+0.62d^2a_0^{12/5}\right)^{5/6}}\right\} - 1\right]^{-1} \quad (4)$$

where b_0^2 defines Rytov variance as well as d means spherical wave diameter [24].

Fig. 4(a)-4(d) indicate measured BER for varied fiber link with a fixed FSO range of 100 m at mode 0 and mode 1 in DS and US transmission for distinct codes.

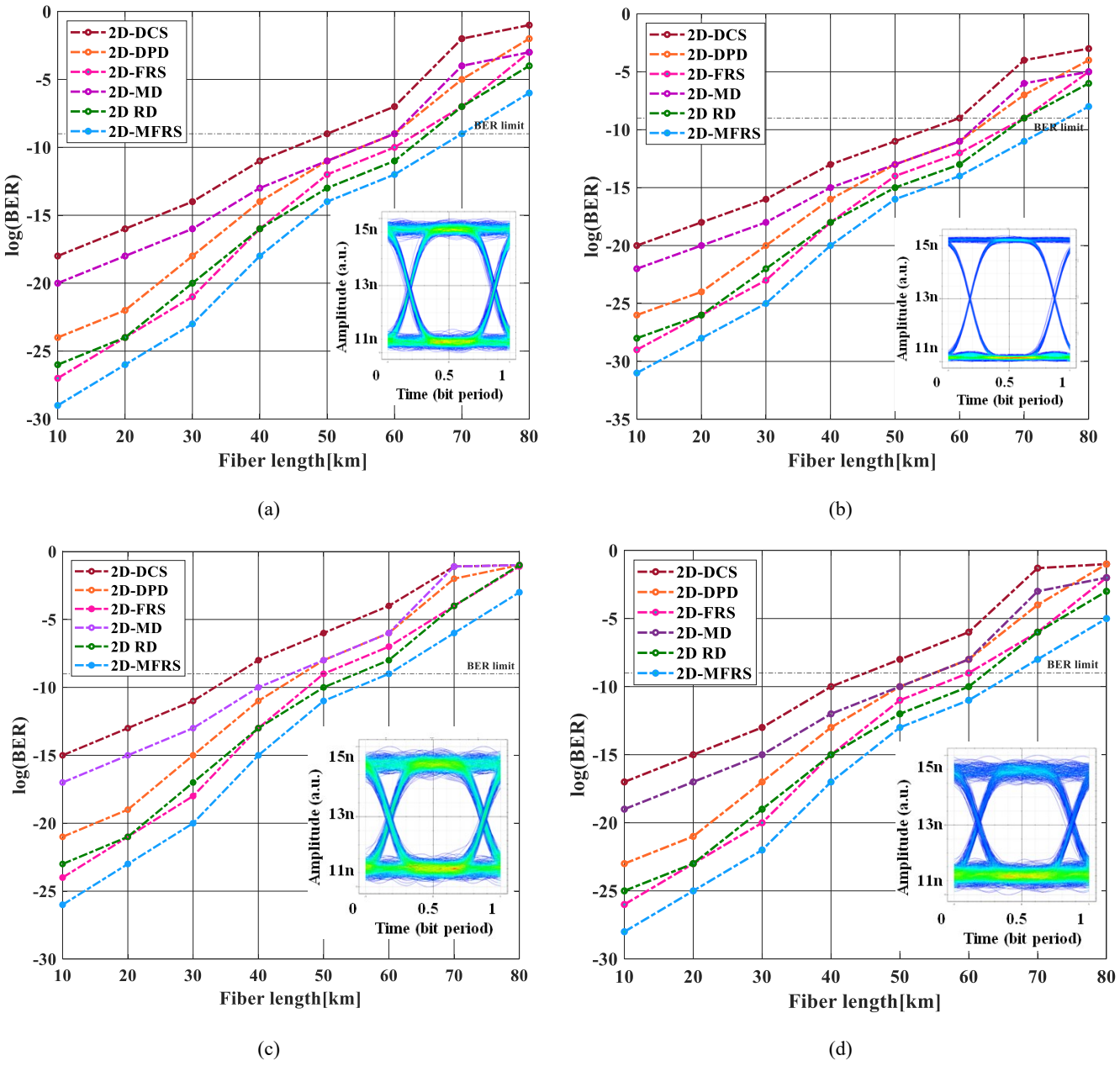

Fig. 4. Measured BER for varied fiber length at fixed 100 m FSO range of (a) DS mode 0, (b) US mode 0, (c) DS mode 1 and (d) US mode 1 signals considering various OCDMA codes; Insets: corresponding eye patterns for 2D-MFRS code at 10^{-9} BER (color online)

As shown in figures, 2D-MFRS code performs best over other codes for varied transmission length at 40/40Gbps transmission rate for mode 0 followed by mode 1. Fig. 4(a) and 4(b) define that maximum fiber length of 70 and 75 km for DS and US transmission respectively, at mode 0 for 2D-MFRS code. Also, for DS and US transmission, maximum fiber length of 60 and 65 km fiber distance can be obtained respectively, at mode 1 for 2D-MFRS code as depicted in Fig. 4(c) and 4(d).

Moreover, wide eye opening means clear received signal, however, distorted signals are observed for eye closure patterns. Table 5 indicated the maximum achievable fiber length for DS and US transmission having different codes. From table it is clear that out of various 2D codes, MFRS code provide maximum fiber length which is followed by RD, FRS, DPD, MD and DCS code considerably.

Table 5. Maximum obtained fiber length in DS and US transmissions for different modes and codes @10^{-9} BER

Codes	Max. fiber length (km)			
	DS		US	
	Mode 0	Mode 1	Mode 0	Mode 1
2D- dynamic cyclic shift (DCS)	50	35	60	45
2D-multi-diognal (MD)	60	45	63	55
2D- diluted perfect difference (DPD)	60	47	65	55
2D- fixed right shifting (FRS)	63	50	70	60
2D-randon diagonal (RD)	65	55	70	63
2D-MFRS	70	60	75	65

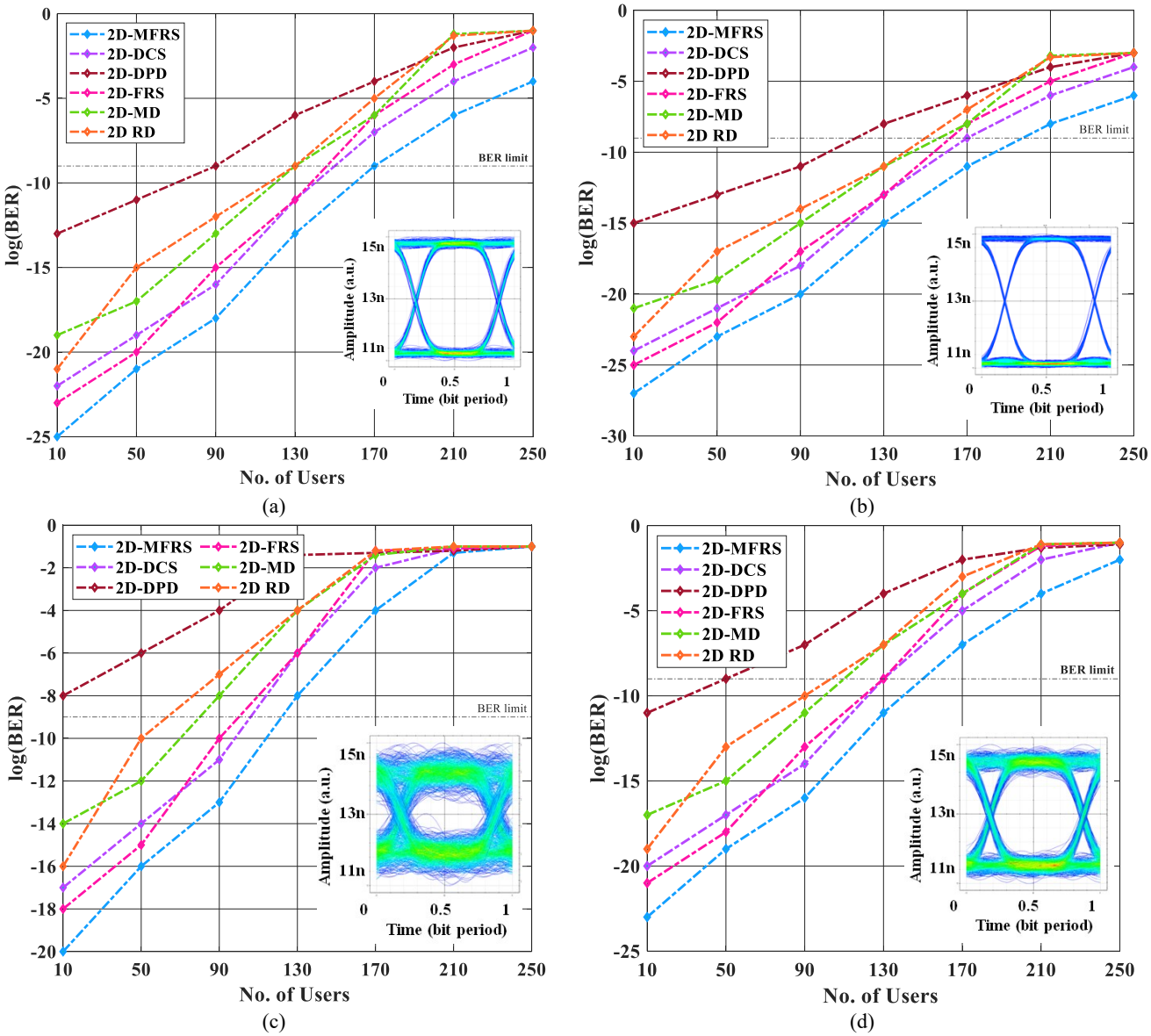

Fig. 5. Measured BER for various no. of users at 100Gbps for (a) DS mode 0, (b) US mode 0, (c) DS mode 1 and (d) US mode 1 signals having different OCDMA codes over fixed 40 km fiber with 100 m FSO range; Insets: corresponding eye patterns for 2D-MFRS code at 10^{-9} BER (color online)

Fig. 5(a)-5(d) illustrate measured BER for various no. of users over 100 m FSO with 40 km fiber at 100 Gbps transmission rate operate at mode 0 and mode 1. As seen from figures, out of all codes 2D-MFRS code shows best performance in terms of sustaining maximum number of end users. Fig. 5(a) and 5(b) indicate that at mode 0, DS and US transmission signals can handle maximum 170 and 190 respectively, for 2D-MFRS code at BER limit. Also,

for the same code, DS and US transmission signals operating at mode 1 can sustain highest 130 and 150 users respectively, as depicted in Fig. 5(c) and 5(d). It is clear that after out of all 2D OCDMA codes, MFRS code depicts supreme performance over DCS, FRS, MD, RD and DPD codes. Besides this, the obtained eye patterns also strengths the above statements.

Table 6 indicates the maximum number of users handled by the proposed architecture for DS and US transmission having different codes. From table it is clear that out of various 2D codes, MFRS code provide maximum users which is followed by DCS, FRS, MD, RD and DPD codes considerably. Besides this, Table 7 defines various performance parameters of all DS and US wavelengths operating at mode 0 and mode 1.

Furthermore, gain, noise figure as well as optical SNR are given as [8,23]:

$$G = 10log_{10}(Output\ power/Input\ Power)\ dB \quad (5)$$

$$NF = 10log_{10}(Input\ SNR/Output\ SNR)\ dB \quad (6)$$

and

$$OSNR = Signal\ Power(dB) - Noise\ Power(dB) \quad (7)$$

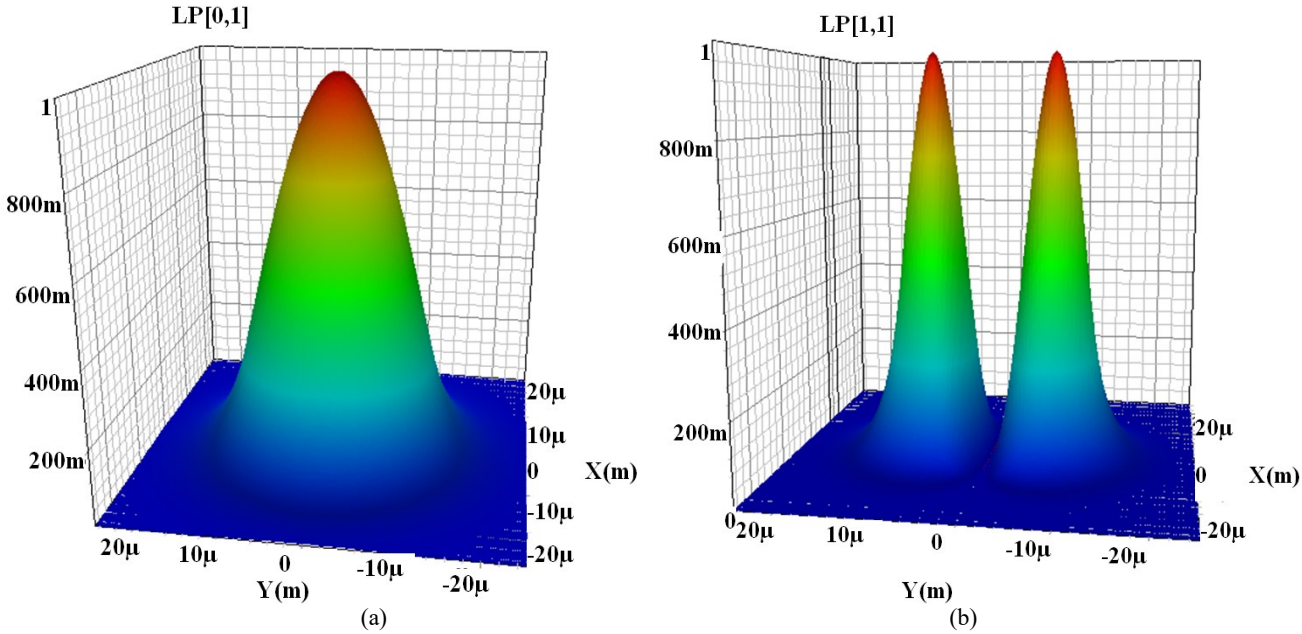

Fig. 6. 3D Obtained modes at receiver (a) mode 0 and (b) mode 1 (color online)

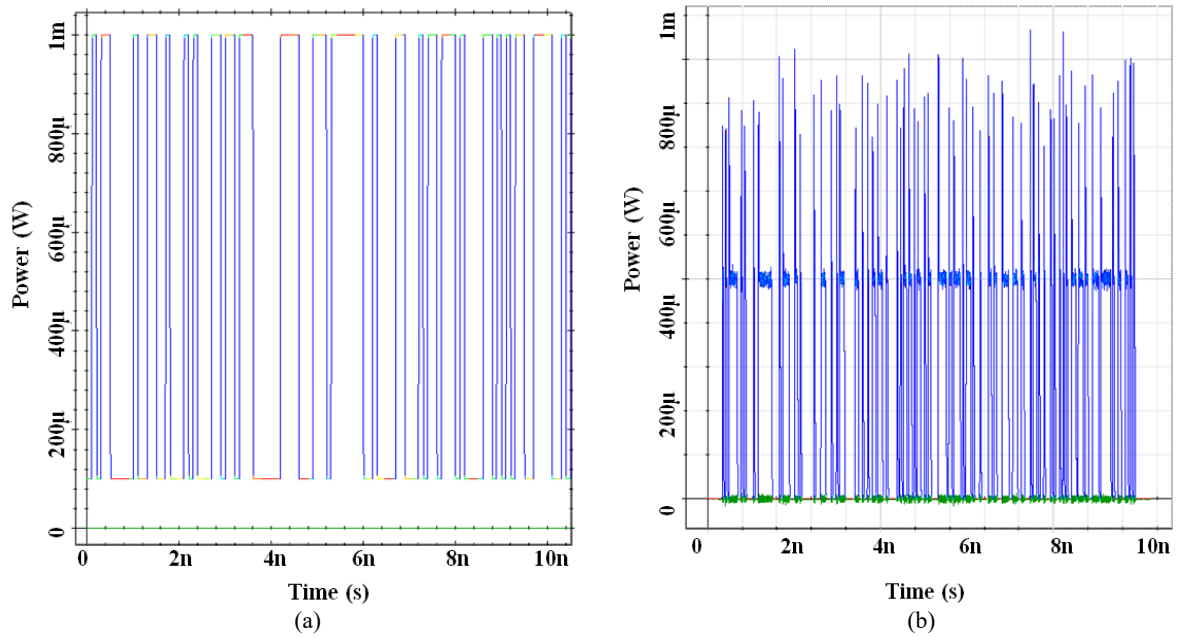

Fig. 7. Obtained timing diagrams (a) before and (b) after transmission over 10 km fiber+100 m FSO range

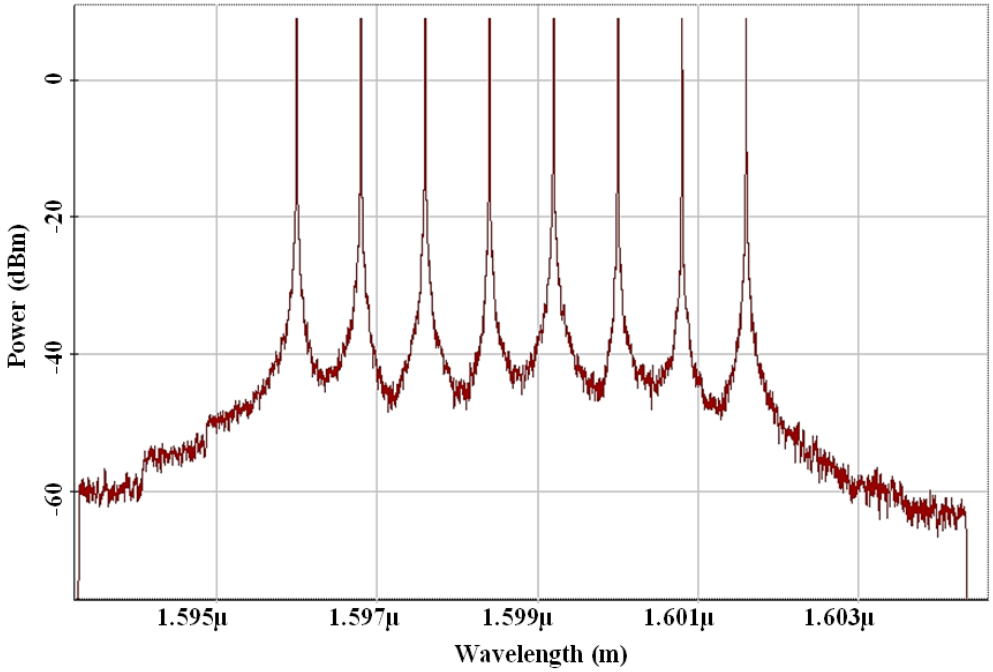

Fig. 8. Obtained optical spectrum after 10 km fiber+100 m FSO range

Fig. 6 indicates the obtained 3D MDM modes i.e. mode 0 and mode 1. Fig. 7 indicates the timing diagrams of the obtained output at receiver. Also, Fig. 8 indicates optical spectrum of the mode signals after 10 km fiber and 100 m FSO link.

Table 6. Maximum no. of users in DS and US transmission at 100 Gbps throughput for different modes and codes @10^{-9} BER

Codes	Max. users			
	DS		US	
	Mode 0	Mode 1	Mode 0	Mode 1
2D- DPD	90	<10	100	50
2D-RD	130	60	140	100
2D-MD	130	80	160	110
2D-FRS	140	100	165	130
2D-DCS	145	110	170	130
2D-MFRS	170	120	190	140

Table 7. Analysis of proposed architecture for DS and DS wavelengths

Transmission	Wavelength (nm)	Mode 0				Mode 1			
		NF (dB)	G (dB)	Optical SNR_i (dB)	Optical SNR_o (dB)	NF (dB)	G (dB)	Optical SNR_i (dB)	Optical SNR_o (dB)
DS	1596	2.2	-3.4	104	103	2.5	-3.6	101	100
	1596.8	2.2	-3.5	102	101	2.5	-3.7	99	98
	1597.6	2.3	-3.6	100	99	2.6	-3.8	97	96
	1598.4	2.5	-3.8	98	97	2.7	-3.9	95	94
	1599.2	3.4	-4.0	103	102	3.8	-4.2	100	99
	1600	3.6	-4.2	102	101	3.8	-4.4	100	99
	1600.8	3.7	-4.3	101	100	3.9	-4.5	99	98
	1601.6	3.8	-4.2	100	99	3.9	-4.4	98	97
US	1527.2	1.4	-3.1	105	104	1.5	-3.3	101	100
	1528	1.5	-3.1	104	103	1.6	-3.3	101	100
	1528.8	1.4	-3.2	103	102	1.6	-3.4	100	99
	1529.6	1.6	-3.4	102	101	1.9	-3.3	100	98
	1530.2	1.5	-3.1	103	102	1.7	-3.3	100	98
	1531	1.4	-3.0	102	101	1.7	-3.2	99	97
	1531.8	1.4	-3.2	101	100	1.8	-3.4	100	98
	1532.6	1.5	-3.3	100	99	1.6	-3.5	99	97

Table 8. Comparison of various OCDMA codes

Code	Code length	Total no. of subscribers	Code weight	Cross-correlation	Complexity
DCS [29]	30	30	4	<1	Medium
2D-FRS [25]	12	63	3	<1	Medium
RD [30]	34	30	4	variable	Low
2D ZCC/MD [31]	91	30	3	0	Medium
2D-DPD [32]	2	52	4	<1	High
2D-MD [32]	33	30	4	0	Medium
2D-DCS [33]	30	30	4	≤1	High
Modified quadratic congruence [8]	12	68	4	1	High
2D-MFRS [This work]	12	63	3	<1	Medium

Table 9. Comparison of various PON based designs

Architecture	Transmission	Topology	Max. fiber range (km)	No. of channels	Throughput/ channel (Gbps)	Scalability	Wireless range (m)	Cost
Add/drop multiplexer [34]	Bidirectional	Hybrid ring-tree	26	not defined	1.25	Low	not used	High
WDM [18]	Unidirectional	Hybrid ring-tree	100	not defined	60	Medium	not used	Moderate
TWDM-PON [3]	Unidirectional	Ring	not defined	not defined	10	Low	not used	Moderate
TDM/FSO [35]	Bidirectional	Ring	25	not defined	10	Low	not defined	Low
Dense wavelength division multiplexing [36]	Unidirectional	Hybrid ring-star	150	not defined	15	Medium	not used	Low
OCDMA-PON [23]	Bidirectional	Wheel	1.6	10	10	Medium	not used	Moderate
This work	Bidirectional	Hybrid ring-mesh	75	16	100/100	High	2800 (FSO)	Moderate

Tables 8 and 9 depict that out of all codes and designs, the proposed new 2D-MFRS code and proposed architecture of hybrid ring-mesh based integrated MDM-NGPON/FSO system indicate best performance.

4. Conclusion

A symmetric 16×100Gbps hybrid ring-mesh topology based integrated MDM-NGPON2/OCDMA PON system incorporating two donut modes 0 and 1 is reported. It is concluded that the downstream and upstream transmission signals can be transmitted successfully over fixed fiber length of 40 km with 1000 m to 2800 m FSO range under weak-to-strong turbulent with combined effect of fog, snow and rain weather condition. Also, the fiber length can be extended to 60-75 km in the proposed architecture using 2D-MFRS code at fixed FSO range of 100 m at 40/40 Gbps data rate. Besides this, at symmetric 100 Gbsp traffic rate, the architecture can supports 120-190 users using 2D-MFRS code as compared to other codes. High gain, low noise figure and high OSNR are also obtained in the performance analysis of the system. The comparison performance of the proposed work in terms of code and architecture illustrates its superior performance over others. In future, this architecture can be used for NG-PON3 basics 5G fronthaul/backhaul network applications.

References

[1] I. Dias, L. Ruan, C. Ranaweera, E. Wong, Opt. Fiber Technol. **75**, 103191 (2023).
[2] C. L. M. P. Plazas, A. M. de Souza, D. R. Celino, M. A. Romero, Opt. Fiber Technol. **76**, 103244 (2023).
[3] Z. Tan, C. Yang, Z. Wang, J. Light. Technol. **35**, 4526 (2017).
[4] K. I. Kitayama, X. Wang, N. Wada, J. Light. Technol. **24**, 1654 (2006).
[5] P. Rajasekaran, G. Ganesan, M. Murugappan, Frequenz **76**, 97 (2022).
[6] R. Matsumoto, T. Kodama, S. Shimizu, R. Nomura, K. Omichi, N. Wada, K. I. Kitayama,

J. Light. Technol. **32**, 1132 (2014).
[7] Y. Cao, C. Gan, Optik **123**, 176 (2012).
[8] M. Kumari, R. Sharma, A. Sheetal, Opt. Quantum Electron. **52**, 1 (2020).
[9] P. Bishal, J. Oshima, Y. Morizumi, H. Kobayashi, K. Iwashita, 2017 Opto-Electronics Commun. Conf. OECC 2017 Photonics Glob. Conf. PGC 2017 **10**, 252 (2018).
[10] S. Chaudhary, X. Tang, X. Wei, AEU - Int. J. Electron. Commun. **93**, 208 (2018).
[11] A. Amphawan, S. Chaudhary, V. Chan, Opt. Commun. **431**, 245 (2019).
[12] P. Vijayakumari, M. Sumathi, Results Phys. **14**, 102503 (2019).
[13] P. Lafata, J. Vodrazka, Elektron. Ir Elektrotechnika **19**, 93 (2013).
[14] A. Zentani, N. Zulkifli, A. Ramli, Opt. Fiber Technol. **73**, 103038 (2022).
[15] C. H. Yeh, F.-Y. Shih, G.-K. Chang, S. Chi, Opt. Express **16**, 4494 (2008).
[16] Y. Gong, C. Gan, C. Wu, R. Wang, Telecommun. Syst. **57**, 327 (2014).
[17] P. Lafataand, J. Vodrazka, Microw. Opt. **48**, 2611 (2006).
[18] S. Singh, S. Singh, Photonic Netw. Commun. **35**, 325 (2018).
[19] A. K. Garg, V. Janyani, B. Batagelj, N. H. Zainol Abidin, M. H. Abu Bakar, Opt. Fiber Technol. **61**, 102422 (2021).
[20] C. H. Yeh, C. W. Chow, C. S. Gu, B. S. Guo, Y. J. Cheng, J. H. Chen, Electron. Lett. **54**, 1228 (2018).
[21] S. B. Ahmad Anas, F. H. Hamat, S. Hitam, R. K. Z. Sahbudin, Photonic Netw. Commun. **23**, 33 (2012).
[22] H. Emami, M. A. Balafar, Opt. Fiber Technol. **79**, 103341 (2023).
[23] M. Kumari, V. Arya, H. M. R. Al-Khafaji, Photonics **10**, 329 (2023).
[24] V. Arya, M. Kumari, H. M. R. Al-Khafaji, S. A. Aljunid, Symmetry (Basel) **15**, 739 (2023).
[25] H. Yousif Ahmed, M. Zeghid, W. A. Imtiaz, Y. Sharief, A. Sghaier, Optik **185**, 746 (2019).
[26] M. Kumari, V. Arya, Opt. Quantum Electron. **56**, 546 (2024).
[27] M. Kumari, V. Arya, Opt. Quantum Electron. **55**, 124 (2023).
[28] M. Kumari, M. Banawan, V. Arya, S. K. Mishra, Photonics **10**, 1384 (2023).
[29] T. H. Abd, S. A. Aljunid, H. A. Fadhil, J. Opt. Commun. **32**, 263 (2011).
[30] S. Chaudhary, A. Sharma, X. Tang, X. Wei, P. Sood, Wirel. Pers. Commun. **116**, 2159 (2021).
[31] R. Matem, S. A. Aljunid, M. N. Junita, C. B. M. Rashidi, I. S. Ahmed, Optik **178**, 1051 (2019).
[32] R. A. Kadhim, H. A. Fadhil, S. A. Aljunid, M. S. Razalli, Opt. Commun. **329**, 28 (2014).
[33] N. Jellali, M. Najjar, M. Ferchichi, H. Rezig, Opt. Fiber Technol. **36**, 26 (2017).
[34] C. Y. Li, C. H. Chang, Z. G. Lin, Photonics **8**, 515 (2021).
[35] C. H. Yeh, Y. R. Xie, C. M. Luo, C. W. Chow, IEEE Commun. Lett. **24**, 589 (2020).
[36] A. Bala, S. Dewra, J. Opt. Commun. **37**, 395 (2016).

*Corresponding author: meetkumari08@yahoo.in